MODELING A RUBBLE FIRE CONSISTING OF COMINGLED LIQUID AND SOLID FUEL

Alexander L. Brown[1], Heeseok Koo[1], Tyler Voskuilen[2], Flint Pierce[2]
[1]Fire Science and Technology Department
[2]Computational Thermal & Fluid Mechanics Department
Sandia National Labs
PO Box 5800
MS 1135
Albuquerque, NM 87185-1135

ABSTRACT

In September of 2014, Sandia National Labs conducted a fire test where over 400 kg of mostly carbon fiber/epoxy composite was mixed with 300 gallons (1100 liters) of jet fuel in a 3-m diameter pan. The test resulted in a very long, slow-burning fire. Recognizing the need to model this type of scenario for accident safety evaluations, we are working to create modeling methods that permit simulation of this complex scenario. Here we describe a two-path approach to the problem. We have been developing liquid-burning models and solid-burning models that can be brought together to resolve the multi-fuel scenario of interest. Our liquid model consists of a volume of fluid (VOF) description of the fuel. Our solid model consists of a Lagrangian-reacting particle capability. Here we illustrate some of the verification and validation activities relating to the separate physics capabilities, primarily focusing on the liquid model. Liquid and solid model capabilities will be brought together at a later date to provide a new computational capability for simulating an important class of accident scenarios.

INTRODUCTION

A test was designed and conducted in September of 2014 that involved the comingling of approximately 300 gallons of jet fuel and 400 kg of mostly carbon fiber/epoxy materials in a 3-m diameter steel pan. The fuel was ignited, and the ensuing fire continued to flame until it was extinguished, more than 14 hours after ignition. The intent of the test was to discover the thermal environment conditions produced by such a fire. The fire was intended to be a scaled-down version of an aircraft fire that is reminiscent of a heavily composite-framed aircraft that creates a rubble fire, including the fuel from the fuel tanks and broken pieces of the aircraft. An open pool fire with just the jet fuel would be expected to burn to completion in about ½ hour, based on projecting a typical fuel burn rate for these conditions. The duration of the burn was remarkable, over 14 hours of active flaming. The test team was not prepared for such a long duration test, and was inhibited by a lack of accurate modeling and simulation tools with which to plan and scope the test.

In response to this lack of simulation capability, a follow-on simulation development effort was conceived that is intended to develop modeling capabilities to simulate the thermal environment caused by a transportation accident of this nature. The data from the September 2014 test serves as a benchmark. The final product of the development activity is a model calculation that serves as a prediction for this type of a scenario.

Certain capabilities were missing from existing fire simulation tools that become necessary for predicting this type of scenario. These include:

- A model for a regressing liquid layer
- Heat transport and reactions of the solid materials

- Joint heat transport between the liquid and solid phases

Models for regressing liquid layers in historical literature normally take the form of a 1-dimensional or 0-dimensional approximation (e.g., Brown and Vembe, 2006, Novozhilov and Koseki, 2004, Prasad et al., 1999). Combustion of a bed of rubble normally leverages theory for transport through porous media. Non-reacting media are commonly used in combustion environments (e.g. Abdul Mujeebu et al., 2009). Combustion in fluidized beds has been relatively heavily studied (e.g. Basu, 1999). Reacting fixed bed media are also modeled in historical studies (e.g. Bryden and Ragland, 1996).

To simulate the problem of interest, a regressing liquid layer model needs to function in a radiating, convecting, and conducting environment. Multi-phase methods normally do not have particular difficulty with convection and conduction problems; however, we have not come across instances of a radiative evaporation model that permits predictive simulation of a regressing pool fire. Notably, there have been recent tests of the flow characteristics of fuels in a burning pool configuration that could make a good validation dataset. No instances of simulation comparisons to these data have been demonstrated yet.

This paper focuses on the implementation of a Volume of Fluid (VOF) method in a reacting fire computational fluid dynamics (CFD) code. The short-term objective is to build confidence in the quantitative accuracy of the flow solution methods, such that they can be extended to the burning environment. The fire prediction tool needs a method for predicting the location of the pools surface, and this exercise is a step towards having confidence in the model for this component of the problem. We discuss the unique aspects of the implementation methods, which are an extension of historical methods. We are implementing the VOF in SIERRA/Fuego, a generalized reacting CFD capability developed for severe- and high-consequence analysis of reacting flows. We illustrate the model through a validation-like exercise where the predictions are compared to some measured data from the literature.

METHODS

VOF methods were first proposed and the term was coined by Hirt and Nichols (1981). They indicated that there are other historical methods for simulating multi-phase problems, including Marker Particles, Line Segments, and Height Functions methods. In some ways, VOF is a more sophisticated method than those historical methods. Marker Particles are still found in current research reports, but the other two methods have since diminished in use. The heart of the VOF method is the equation for the fraction of liquid in a cell 'F'. In Cartesian 3-dimensional representation, the equation for F is:

$$\frac{\partial F}{\partial t} + u\frac{\partial F}{\partial x} + v\frac{\partial F}{\partial y} + w\frac{\partial F}{\partial z} = 0$$

This equation expresses the conservation of fluid phases and the advective transport. This equation can be modified to include source and sink terms to accommodate non-idealizations like compressibility of fluids, evaporation, etc. F is unity if a cell is full of liquid, and zero if it is empty (gas only). If in a computational cell, F is between 1 and 0, a solid-gas interface exists at the cell. Based on the F variable alone, it is not possible to know the precise shape or orientation of the interface at resolutions lower than the local mesh resolution. The variable F provides the Eulerian solver with a method to select the active fluid properties (including density, viscosity, and heat capacity) that are required for computing the transport in the computational cell.

This method has drawbacks, particularly for small drops and fine-liquid structures. When the size of the relevant liquid features is comparable to the mesh size, some particular features of

the liquid (such as surface area or surface curvature) are not represented accurately. Lack of knowledge regarding interface inside a computational cell complicates the application of surface physics, like surface tension and evaporation, because there is model uncertainty in the dimensions, shape, and orientation of the interface that can be a major source of error, depending on the problem specifics. Resolution of interface features is often improved by refining the mesh in the region near the interface to better resolve the surface. There also needs to be a model for the transport and fluid properties in the transitional cells. This normally involves a weighted function of the phase properties. When reconstructing an interface, it is necessary to have a concept of the curvature of the surface to appropriately vector the surface force. This can be modeled based on a fit involving neighboring computational cells, with the interface resolution being dependent on the resolution of the mesh. It can also be modeled with other methods described in the literature. Some of the disadvantages are remedied with level-set capabilities; however, those are often challenged by poor mass conservation, and consequently not considered for this application.

For modeling more than just a moving interface, modifications are made to the basic VOF equation. In the case of this application, we have implemented the following modifications:

- Geometric advection using interface compression for improved surface definition
- Evaporation by deviation from saturation temperature method (Hardt and Wondra, 2008)
- Pressure stabilization through a pressure diffusion term (Tukovic and Jasak, 2012)
- Surface tension and gravity body forces, using a velocity correction factor (Francois et al., 2006)

A series of verification tests has been used to demonstrate the adequacy of the numerical implementation. Tests include:

- Basic advection
- Planar advection
- Circle advection
- Hollow square advection
- Shearing advection

Complete verification test documentation is available in Koo et al. (2017). The scenarios tested for verification provide confidence in the implementation of the basic advection capability. Here the circle advection test is illustrated. A divergence-free shearing flow has been used by many authors, but was originally described by Rider and Kothe (1998). This test uses a square 2D domain with a velocity field of:

$$u =< \cos(\pi x) \sin(\pi y), -\sin(\pi x) \cos(\pi y) >$$

The sign reverses after 1000 time steps, resulting in the theoretically perfect reconstruction of the circle. Mesh convergence was tested at a constant Courant Friedrichs Lewy (CFL) number and at a constant time step (Table 1). This means that the mesh spacing and time step were changed simultaneously, and the number of time steps increased accordingly. The computed order of convergence is 1.02, which is consistent with the upwind advection scheme used. Results of different mesh resolutions are found in Figure 1.

Table 1. Mesh convergence studies for reversing vortex test

Mesh	Time Step	CFL	Final Shape Error
100x100 (001 m)	2.5 ms	0.25	10.85%
200 x 200 (0.005 m)	1.25 ms	0.25	5.29%
400 x 400 (0.0025 m)	0.625 ms	0.25	2.64%

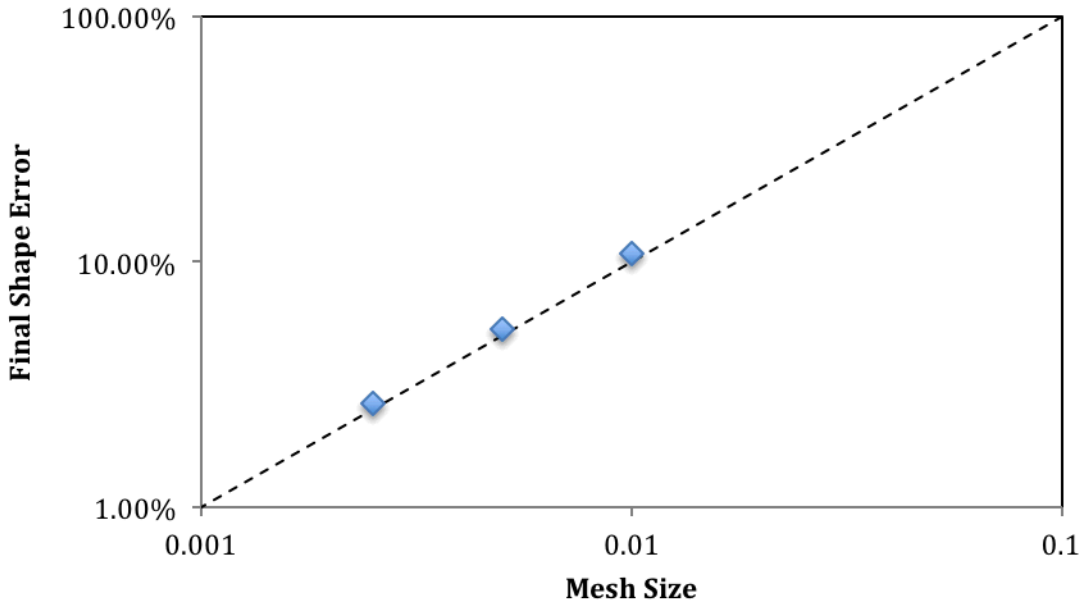

Figure 1. Mesh convergence study, showing line for 1st order convergence. Three points correspond to the cases listed in Table 1

A graphical representation of the final circle is shown in Figure 2. The fine mesh does a respectable reconstruction of the circle, and the coarse mesh exhibits significant diffusion upon reconstruction.

Figure 2. Final circle shape with a) coarse, b) medium, and c) fine meshes

As a further test of the VOF implementation, comparisons to data provide confidence in the accuracy of the models implemented. One classical scenario that provides a good challenge for multi-phase simulations is the dam burst scenario, which involves the rapid removal of a dam-like structure (gate valve) and the subsequent re-adjustment of the fluid due to the gravity force.

The experimental test of Kleefsman et al. (2005) was simulated by Crespo et al. (2011), and seems to be a good test problem. It involves a 3.22-m long tank with a 1-m square cross-section. The initial water height was 0.55 m, and the length 1.228 m. A rectangular obstruction was located 0.6635 m from the down-stream end, and was 0.161-m high, 0.403-m wide, and 0.16-m in the length direction. Heights were sampled at 0.582, 1.732, and 2.228 m downstream, as indicated in Figure 3.

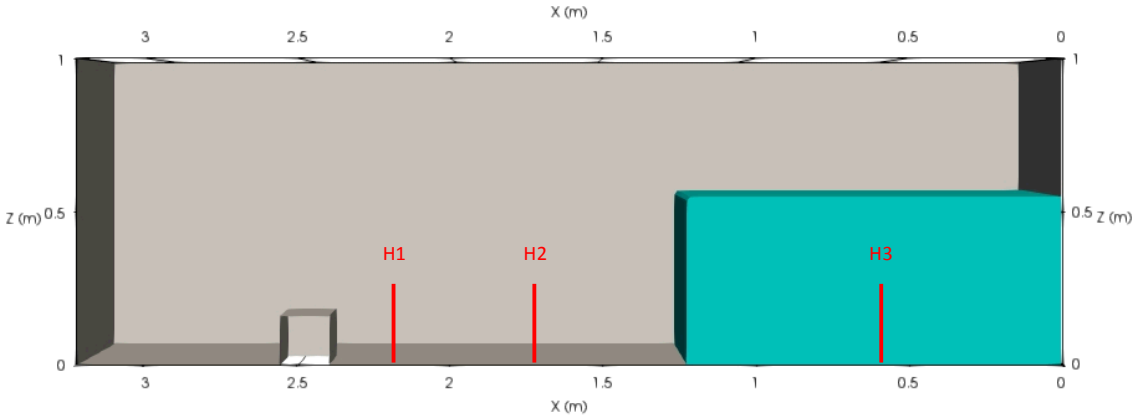

Figure 3. An illustration of the initial dam burst scenario with measurement points annotated

The simulation assumed a gas density of 1 kg/m^3, fluid density of 1000 kg/m^3, surface tension of 0.07 N/m, liquid viscosity of 0.001 Pa-s, gas viscosity of 1.98e-5 Pa-s, and a contact angle of 45º. A coarse mesh was formed, and progressive refinements were performed in Cubit software to split the coarse mesh an integral number of times, resulting in the mesh refinement as illustrated in Table 2. The mesh was very close to orthogonal and square, with the maximum aspect ratio for the coarse mesh being 1.087. The time step was managed to keep the CFL number mostly below 1.0, as indicated in the table. Typical maximum CFL numbers were between 0.1 and 0.5 at each time step.

Table 2. Dam burst meshes

#	Mesh	Nodes	Nominal Mesh Spacing	Time Step (s)
1	coarse	28,600	0.05000 m	0.00250
2	med	216,400	0.02500 m	0.00125
3	fine	716,500	0.01667 m	0.00100
4	xfine	1,682,000	0.01250 m	0.00100
5	xxfine	3,266,300	0.01000 m	0.00050
6	xxxfine	5,622,400	0.00833 m	0.00050
7	xxxxfine	8,903,500	0.00714 m	0.00050

Kleefsman et al. (2005) and Crespo et al. (2011) demonstrate model accuracy by comparing the height of the fluid at the above-mentioned downstream locations. Data were extracted from Crespo et al. (2011) and are replicated in Figure 4 through Figure 6, along with predictions from the newly implemented model. Kleefsman et al. (2005) and Crespo et al. (2011)

use different conventions to identify downstream measurement locations. This effort follows the convention used in Crespo et al. (2011).

RESULTS AND DISCUSSION

Figure 4 shows fluid height predictions and data for the H1 location, which is just up-stream of the obstruction. Models track the data well up to one second. At later times, the arrival of the wave peaks is slightly delayed compared to the data. As the mesh is refined, the magnitude of the delay generally decreases. Figure 5 shows H2 location results, which exhibit similar results to the H1 location. One difference is that the arrival of the first peak is slightly in advance of the data for the highest resolution model case. Figure 6 shows the H3 location results. This location is inside the initial liquid column, so at early times the liquid level is high. Early time simulation results all are similar to the data, diverging at around 2.5 seconds. At that time, there is a reflection wave that arrives at a very close time for the data and the two refined model simulations. At about 4 seconds, there is a second peak caused by the second reflection of the wave. The peak height tends to be under-predicted, although the two more refined scenarios correspond better to the data. Peak height was calculated numerically by identifying the maximum height where the volume of fluid was at least 0.5. Locations were determined by the variable clipping algorithm in Paraview (v. 5.1.2), which presumably locates this precise height using a linear interpolation function. The early peaks in the xxfine predictions for the H1 and H2 locations are caused by splash-back, which is likely ignored in the data and is under-resolved in the coarser simulations.

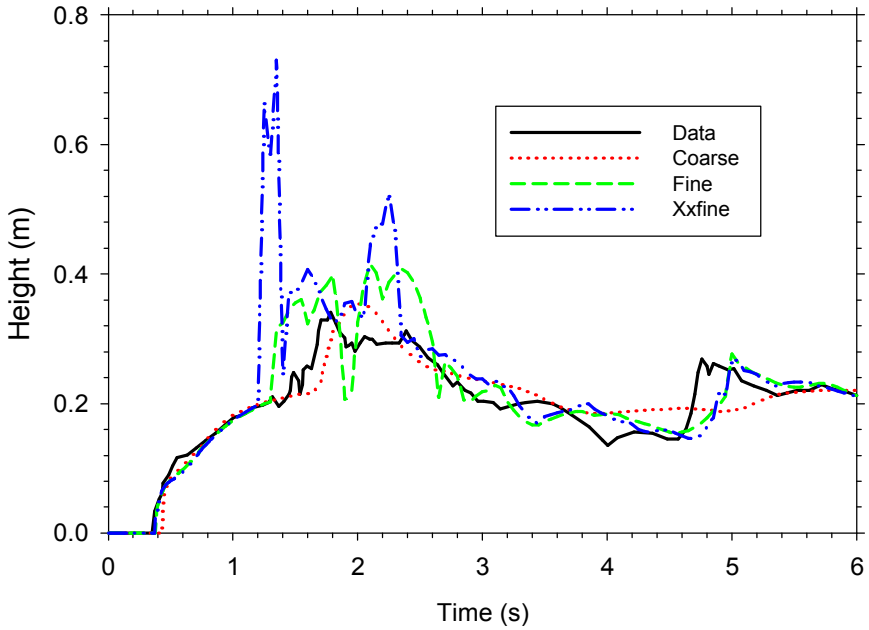

Figure 4. Fluid height results at the H1 location

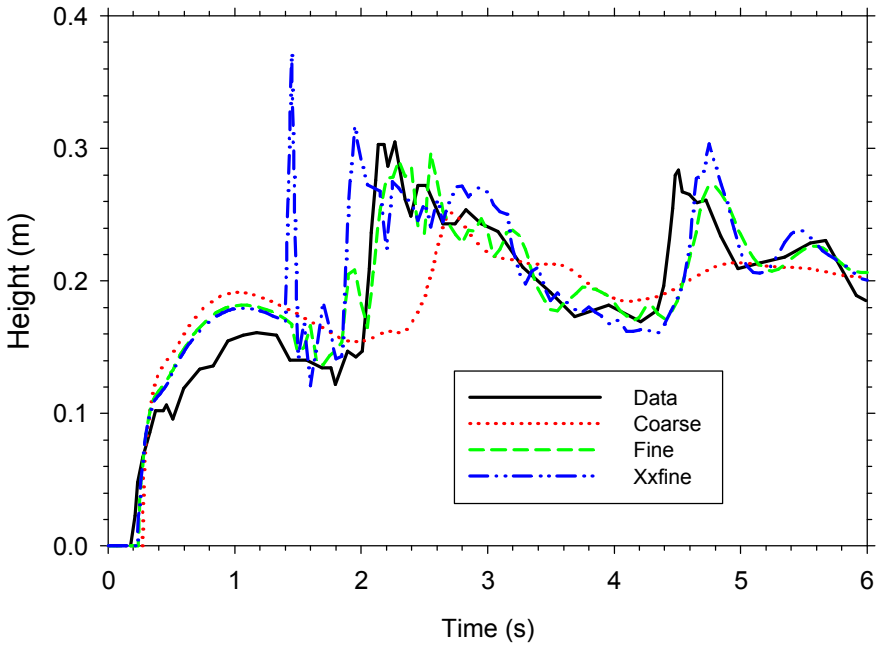

Figure 5. Fluid height results at the H2 location

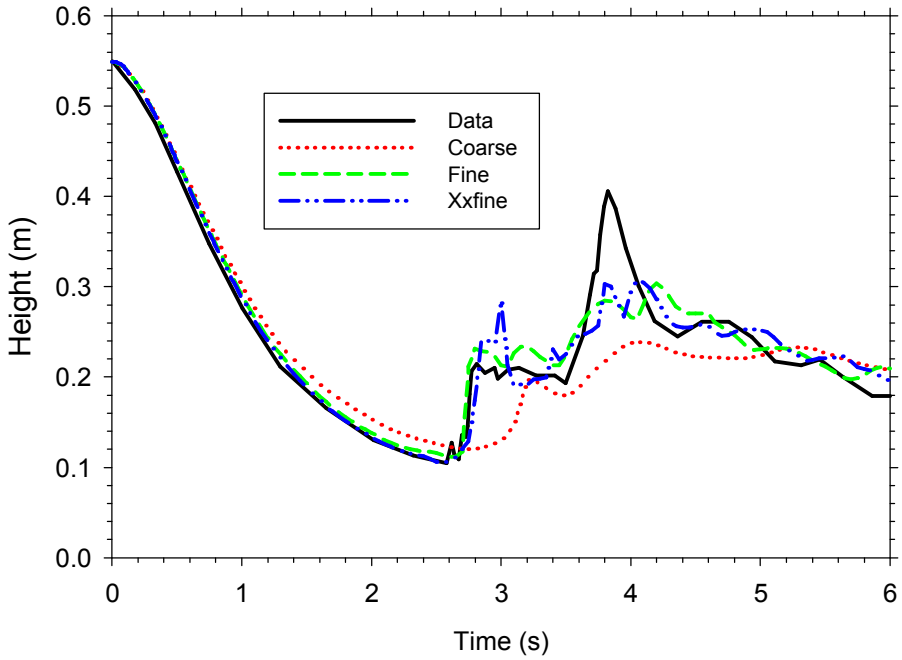

Figure 6. Fluid height results at the H3 location

In addition to the height data, the experiments produced images of the spreading liquid. Crespo et al. (2011) and Kleefsman et al. (2005) extracted images at particular times for comparison with their models. Selected images of the predictions at the same times are provided in Figure 7 and Figure 8. The source material may be consulted for corresponding data images. The images in Figure 7 show predictions for the coarse, fine, and xxfine simulations (all odd-numbered meshes in Table 1). These are arranged with the coarser mesh predictions higher in the image group. At 0.32 through 0.64 seconds, there is a clear difference in the location of the

leading edge of the spreading liquid. The increased refinement scenarios predict a faster spread, which is not particularly unexpected, given that there is improved resolution on the mesh to resolve the small features of the leading edge of a spreading liquid. Features like the drop separation (at 0.64 sec) and gas bubble formation (2.0 seconds) are enhanced for the finer scenarios.

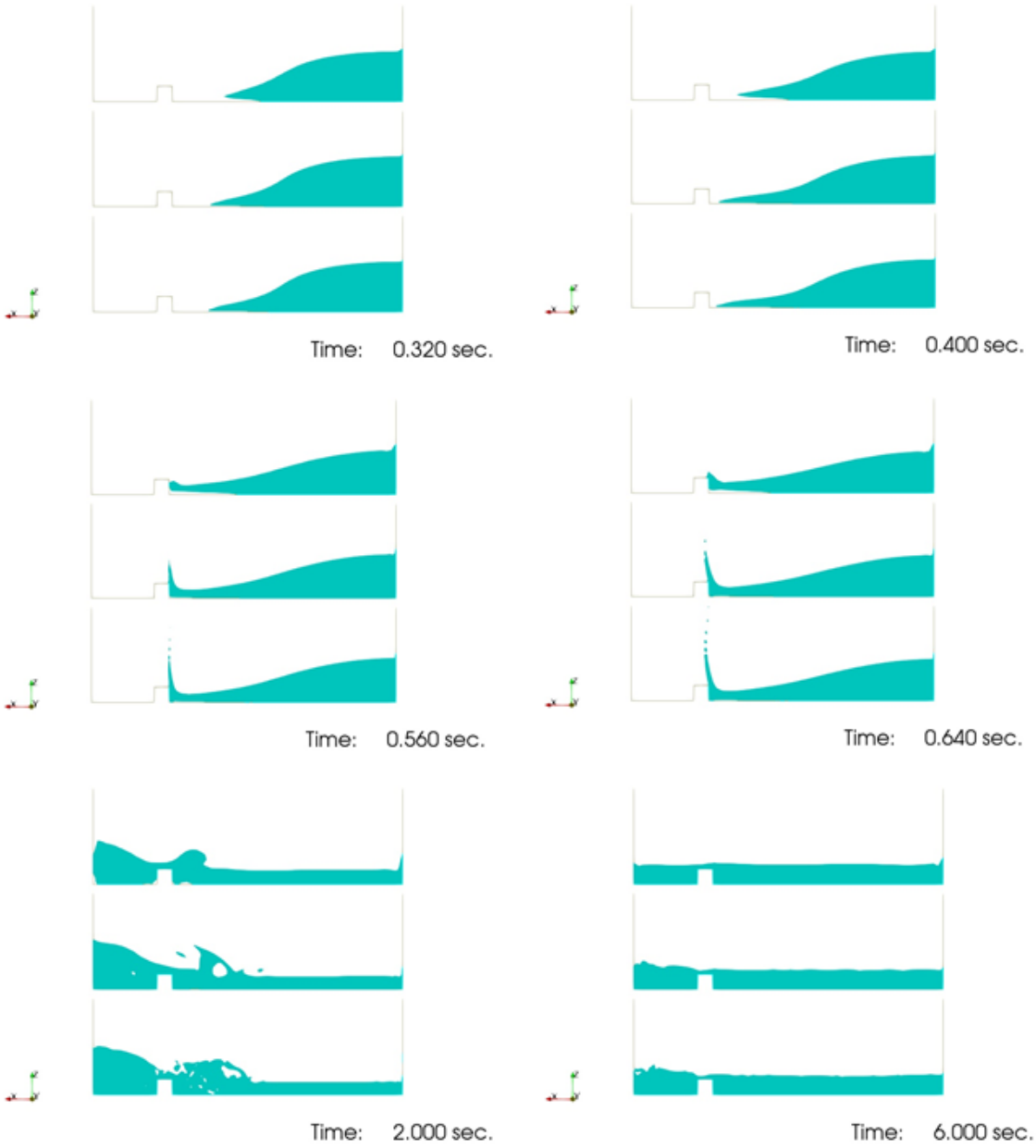

Figure 7. Center-plane images of the fluid at various times for three mesh resolutions; coarse, fine, xxfine (top to bottom)

Figure 8 shows 3D views of the flow and include one higher level of resolution. They show a similarity in answer, and improved similarity with increasing resolution. Predictions at early times are similar. Note at 2.0 seconds, the finest scenario exhibits the greatest amount of surface detail.

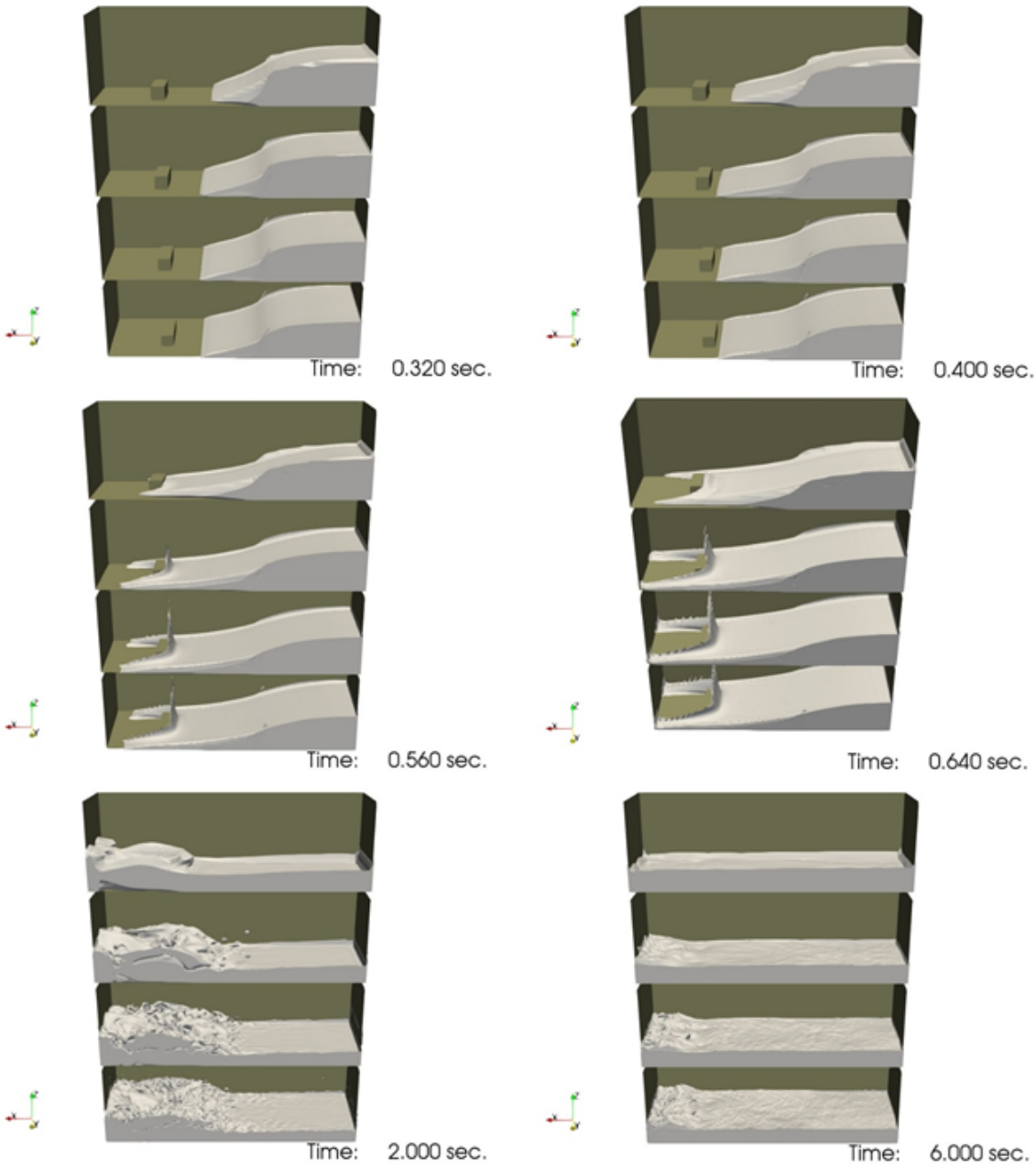

Figure 8. Images of the rendered fluid at various times for four mesh resolutions; coarse, fine, xxfine, xxxxfine (top to bottom)

The leading edge is extracted at similar times for the various mesh resolutions to help demonstrate the mesh convergence of the algorithm. Figure 9 and Figure 10 show the predicted length of spread for either the total node count or the resolved length scale (mesh length unit), both indicated in Table 1. The results exhibit good length-scale convergence for the earlier times, with results showing poorer convergence at later time (0.56 sec.). The 0.64 second results appear convergent, but the fine mesh and above results all agree that the liquid reaches the back (downstream) wall (not an indicator of convergence). The 0.56 second results appear slightly non-convergent, which is probably due to the fact that the spread has to navigate the obstacle at

this time. The flow around the obstacle is likely under-resolved, resulting in increased differences in the flow prediction.

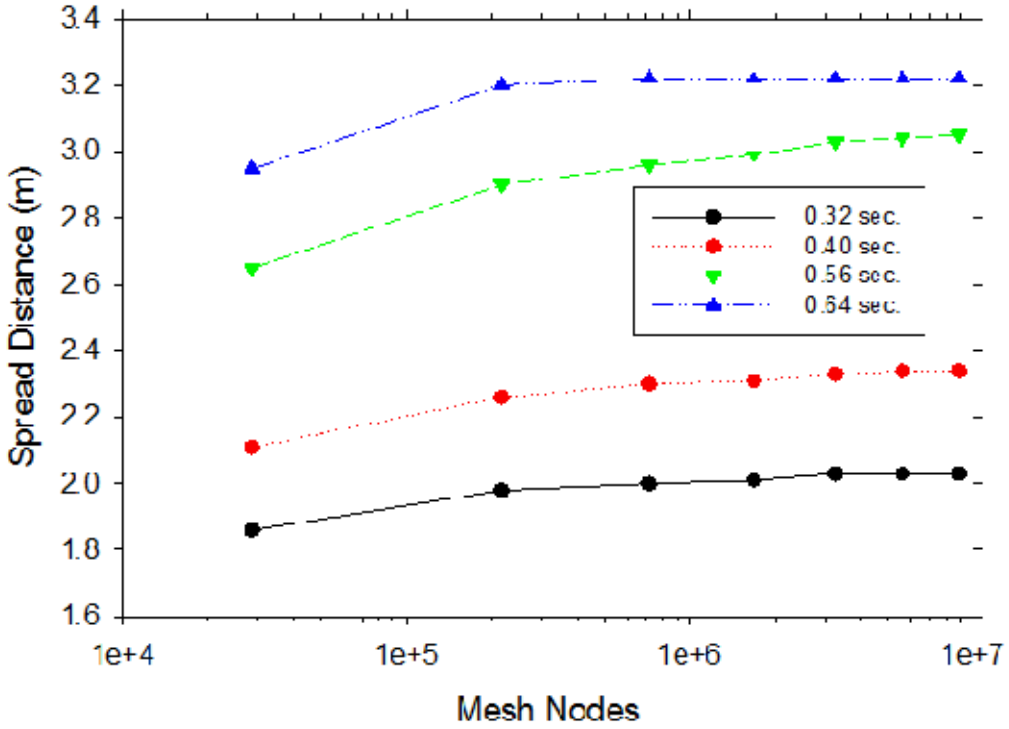

Figure 9. Predicted spread distance for various numbers of mesh nodes

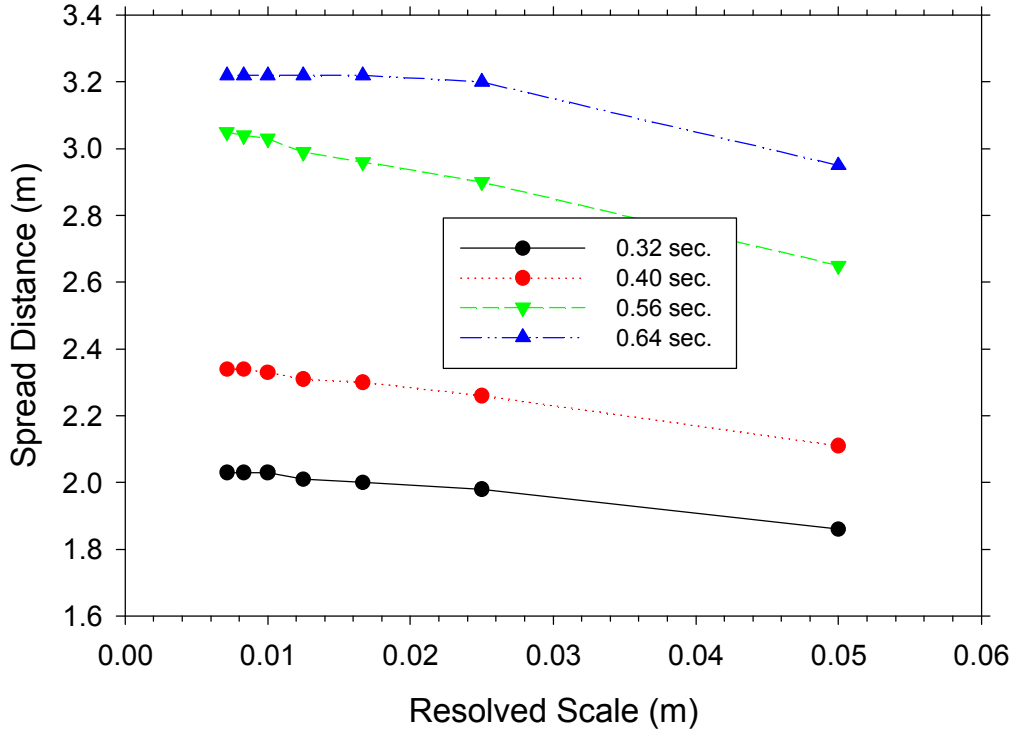

Figure 10. Predicted spread distance versus resolved length scale (mesh spacing)

This simulation exercise provides some confidence in the ability of the implemented multi-phase algorithms to reproduce physical data. The simulations were performed with idealized fluid properties, and give a reasonably adequate representation of the complex behavior of the liquid as determined in the experimental tests. Mesh resolution is shown to affect the quality of the prediction for very coarse meshes. Besides these quantitative simulation issues, there is also the question of the dam removal process and its effect on the initial conditions of the liquid, as well as the temporal component of the removal when compared to the instantaneous assumption made in the model. Given these sources of uncertainty, the model provides a reasonably good reproduction of the measured behavior of the liquid for this scenario.

GENERAL DISCUSSION

The results section depicts a validation exercise for a VOF implementation in a control volume finite element (CVFEM) fluid code. The dynamics of this scenario include significant splashing and, in this regard, are much more significant than is required for the target rubble scenario. This was not necessarily the best validation test for future confidence in the regressing fuel capability, but suggests that the method may be extensible to complex flows. The test lacks evaporation and significant thermal variations. A test of more significance would be a test involving a fuel layer or similar regressing, due to a fire or other heat source above the liquid. The types of data that can be used to validate such a model include classical correlations for fuel burn rate. A recent dataset by Vali et al (2014) measured the flow of liquid in the liquid during a fire. This dataset also represents a good detailed scenario to evaluate for the flow induced in the liquid layer by the heat transport occurring in the liquid during the burn.

A capability that is missing presently to be able to predict the burning behavior of fuels is the radiation coupling. Most CFD codes are not designed to couple the radiation with a multi-phase capability to support fire simulations. Some examples of this type of capability include Hasečić et al (2016), who radiatively couple a liquid-gas system, and Makhanlall and Liu (2010), who couple liquid-solid transition with a radiative solver. We have not found any development or application work in the literature describing a VOF capability for a liquid pool fire simulation. Thus, the solution to the pool simulation capability alone without the rubble mixed in constitutes what is believed to be a unique development for fire modeling applications. A particular challenge with this capability revolves around the predictive behavior of the interface. Figure 11 illustrates graphically the potential behavior of a ray of initial intensity (I_O) that transports through a semi-transparent medium until it is incident on a surface. The surface may induce a reflection (I_R), or it may continue refracted into the liquid layer (I_{Liq}). It can continue to be absorbed by the liquid, or it may interact with a surface below the liquid (I_{Final}). The complexity of the dynamical behavior of the interface challenges implementation in the CFD code, particularly in regard to the reflection and the surface absorption. Our current model employs a gray approximation, and this may be increasingly inadequate for simulating liquid phase transport. Identifying appropriate solutions to this problem is a current activity.

The addition of a rubble burn model will be another unique development associated with this project. Besides being a challenging problem alone, the coupling of a rubble inside and above the liquid layer will be a capability that is not commonly illustrated in historical literature.

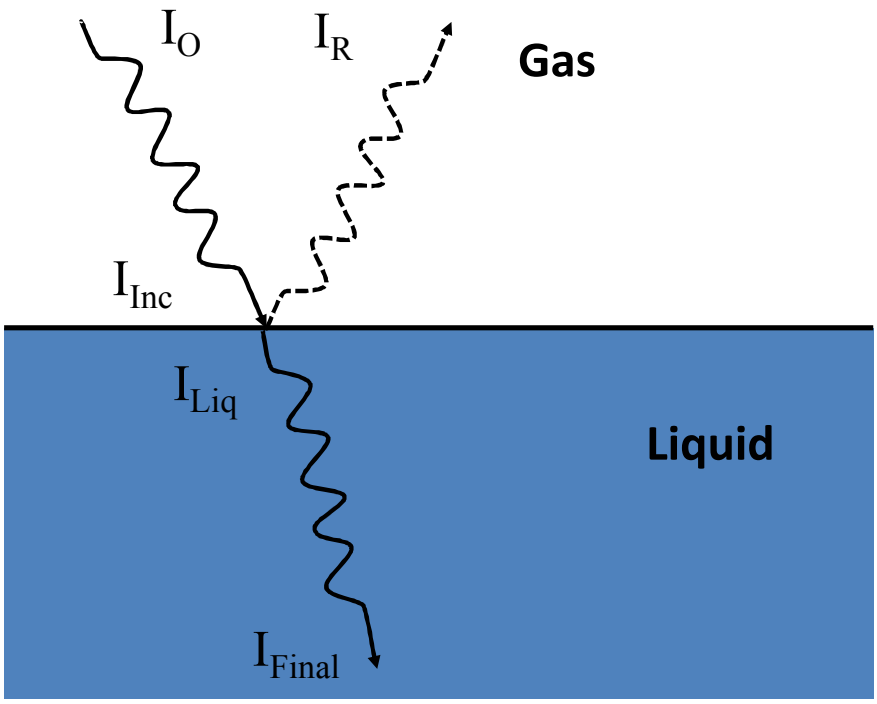

Figure 11. A notional illustration of the fate of incident radiation at a liquid gas interface

CONCLUSIONS

In support of model development to predict a rubble fire involving a mix of solid and liquid fuel, a volume of fluid capability has been implemented in the SIERRA framework in the low-Mach number fire code, Fuego. The numerical implementation is believed to be unique in the assembly of a variety of model components for predicting the behavior of the liquid/gas interface, and in the implementation in a CVFEM framework. The model has been characterized against some historical data. The model gives a reasonable representation of the flow dynamics measured. Further developments are forthcoming that will enable simulation of complex burn scenarios for predicting transportation fire environments.

ACKNOWLEDGMENTS

Sandia National Laboratories is a multimission laboratory managed and operated by National Technology and Engineering Solutions of Sandia, LLC., a wholly owned subsidiary of Honeywell International, Inc., for the U.S. Department of Energy's National Nuclear Security Administration under contract DE-NA0003525.

REFERENCES

1. Brown, A.L., Vembe, B.E., "Evaluation of a model for the evaporation of fuel from a liquid pool in a CFD fire code," Proceedings of the ASME International Mechanical Engineering Congress & Exposition, November 5-10, 2006, Chicago, IL, USA, IMECE2006-15147.
2. Prasad, K.; Li, C.; Kailasanath, K.; Ndubizu, C.; Anath, R.; and Tatem, P.A., "Numerical modeling of methanol liquid pool fires," Combustion Theory and Modelling, v. 3, p. 743-768, 1999.

3. Novozhilov, V. and H. Koseki, “CFD Prediction of Pool Fire Burning Rates and Flame Feedback,” Combust. Sci. and Tech., 176:1283-1307, 2004.
4. Abdul Mujeebu, M., Abdulla, M.Z., Abu Bakar, M.Z., Mohammad A.A., and Abdulla, M.K., “Applications of porous media combustion technology-A review”, Applied Energy 86, 136501375, 2009.
5. Basu, P., “Combustion of coal in circulating fluidized-bed boilers: a review,” Chemical engineering Science, 54, 5547-5557, 1999.
6. Bryden, K.M., and Ragland, K.W., “Numerical Modeling of a Deep, fixed Bed Combustor,” Energy & Fuels, 10, 269-275, 1996.
7. S. Hardt and F. Wondra. Evaporation model for interfacial flows based on a continuum-field representation of the source terms. Journal of Computational Physics, 227(11):5871-5895, MAY 2008.
8. Z. Tukovic and H. Jasak. A moving mesh finite volume interface tracking method for surface tension dominated interfacial fluid ow. Computers & Fluids, 55:70-84, FEB 2012.
9. M. Francois, S. Cummins, E. Dendy, D. Kothe, J. Sicilian, and M. Williams. A balanced-force algorithm for continuous and sharp interfacial surface tension models within a volume tracking framework. Journal of Computational Physics, 213(1):141-173, MAR 2006.
10. Vali, A., Nobes, D.S., and Kostiuk, L.W., “Transport phenomena within the liquid phase of a laboratory-scale circular methanol pool fire,” Combustion and Flame, 161, pp. 1076-1084, 2014.
11. Koo, H., Brown, A.L., Voskuilen, T., and Pierce, F., “Rubble Fire Multi-Phase Model Development,” SAND 2017-9463.
12. W. Rider and D. Kothe, “Reconstructing volume tracking,” Journal of Computational Physics, 141(2):112-152, APR 1998.
13. K. Kleefsman, G. Fekken, A. Veldman, B. Iwanowski, and B. Buchner. A volume-of-fluid based simulation method for wave impact problems. Journal of Computational Physics, 206(1):363{393, JUN 2005.
14. C. Crespo, J. M. Dominguez, A. Barreiro, M. Gomez-Gesteira, and B. D. Rogers. GPUs, a new tool of acceleration in CFD: Efficiency and reliability on smoothed particle hydrodynamics methods. PLOS ONE, 6(6), JUN 2011.
15. Hasečić, A., S. Muzaferija, and I. Demirdžić. "Finite volume method for radiative transport in multiphase flows with free surfaces." Numerical Heat Transfer, Part A: Applications 70.4 (2016): 347-365.
16. D. Makhanlall and L. H. Liu, Second Law Analysis of Coupled Conduction-Radiation Heat Transfer with Phase Change, International Journal of Thermal Sciences , vol. 49, pp. 1829–1836, 2010.